Team Number :	apmcm2103847
Problem Chosen :	A

Research On The Application Of Sub-pixel Edge Detection Technology In The Precision Measurement Of Workpiece Dimensions

Summary

As technology improves by leaps and bounds, the requirements for measurement instruments are increasingly higher. This article introduces edge image segmentation and Canny algorithm and sub-pixel images. The actual length of the part is measured based on the relationship of the calibration plate pixels to the real distance. Finally, the Ramer algorithm is used to fit the image, which then accurately extract the actual data of the image edge profile.

For Question 1, by drawing the subpixel edge contour, it is first necessary to transform the edge subpixel data into the orderly edge contour curve data, considering how to eliminate the interference effect of the edge hairy margin and shadow parts. Two images, Pic1_1 and Pic1_2, are processed in the same way, sharpening the images using the Laplace operator, the image contour smoothed, followed by thresholding of OTSU binarization and Gaussian filtering for denoising, and finally coarse segmentation with the Canny algorithm. Processing Pic1_3 images were taken under conditions that were environmentally complex. The PSO-OTSU algorithm is used to reduce the highlight of the image, and finally the part defect detection and contour repair to obtain the ideal binarized image for contour inspection. Then the subpixel edge detection is to determine whether the image has reached 0.1 pixels, and finally the image edge profile is segmented by the Ramer algorithm.

For Question 2, when measuring the true length of the given parts pictures, measure it according to the calibration version of the given level. The true length of the provided product image is measured according to the calibration board images of three different angles provided.

For image pre-processing, OTSU binarization segmentation, Gaussian filtering denoising, image correction, and Canny algorithm segmentation are required for image preprocessing. The image sharpening of the Laplace operator of the part gives the final segmented part segmentation image. Later, the subpixel-level image segmentation of the calibration board and the parts needs to extract the contour edge of the mark point, improve the precision of the center distance measurement, and the parts need to measure the precision to obtain the pixel circumference of each area of the part. Finally, the true length of each part is measured.

For Question 3, model the two subpixel contour edge data provided in the attachment, analyze the edge contour curve data to fit the straight segment, arc segment or ellipse arc segment, find the segmentation of Edges through Halcon, get the outline

of the line, circle and ellipse according to the read subpixel coordinate data, and finally the center, start position and termination position of the contour everywhere. First, perform contour segmentation on the paper, then perform the Ramer algorithm used in contour fitting, and perform edge contour data extraction.

Key words: Subpixel Detection; Image Segmentation; Ramer Algorithm; Part Measurement; Contour Fitting

Content

1 Introduction

1.1 Question Background

As technology and science grows by leaps and bounds, the demand for intensive reading of work piece parts measurement continues to improve, and the intensive reading requirements of measuring instruments are becoming more and more demanding. In this paper, the edge analysis of the digital image size calculates the image edge profile curve under the subpixel processing.

1.2 Question Restatement

Question 1: For the subpixel edge extraction method and process analysis of 0.1 pixel accuracy or above, the subpixel edge contour boundary of the three images of Annex 1 is extracted and the subpixel point data is converted into the orderly edge contour curve data. The interference effect of the edge hair margin and the shadow part should need to be taken into account. Of the three images, Pic1_3 images taken in complex environments have more interference information. The problem requires extracting the three image edge profiles and drawing different colors, calculating the number of total edge profiles, the total edge contour length of the image coordinate space, the number of points and length of the contour curve, and determining the coordinates of each contour point. Finally, the number of points and points and length data on each curve are calculated.

Question 2: Measured images need to be standard with a point matrix calibration version. On the calibration version, the point diameter is 1mm and the distance between the center of the two points is 2mm.The attachment provided attachment contains three calibration map images taken at different angles and a product image. The length of the total edge profile was calculated by building the model with actual measurements of the edge of the product image profile.

Question 3: Two subpixel contour edge data are provided, and the mathematical model is analyzed and discussed. It is also necessary for the length of each sub-pixel contour edge of the part image segmentation to be calculated. The blue curve starts with the blue number 1 label and outputs the model calculated result data along the direction of the arrow. The green curve starts with the green number 1 label and outputs the model calculated result data along the direction of the arrow. The parameters of the segment segment are written to the table as shown in Annex 3.

2 Model Hypothesis

·Suppose that when extracting the image location point, the point where the most line intersects is the unique center point of the image;

·Suppose that the calibration board height is consistent with the part shooting height.

3 Symbol Description

Table 1 symbol description

Symbol	Explain
ω_k	The proportion of pixels points to the entire image
μ_0	Average gray scale
g	Interclass variance

σ	Standard deviation of the Gaussian distribution
I_i	Pixel distance
Z_i	actual distance

4 Problem Analysis

4.1 For Question 1

To draw the sub-pixel edge contour, first extract the edge contour, and transform the edge subpixel data into the curve data of the orderly edge profile, taking into account how the interference effect of the edge margin and shadow parts can be eliminated. Two images, Pic1_1 and Pic1_2, were processed in the same way, sharpening the images using the Laplace operator, the image contour smoothed, followed by thresholding for OTSU binarization and Gaussian filtering for denoising, and finally coarse segmentation with the Canny algorithm. Processing Pic1_3 images were taken under conditions that are environmentally complex. The PSO-OTSU algorithm was used to reduce the highlight of the image, and finally to detect the part defects and contour repair, to obtain the ideal binarized image for contour inspection..1Then the subpixel edge detection is performed to determine whether the image has reached 0 pixels, and finally the image edge profile is segmented with the Ramer algorithm. Observe Figure 1 for the overall flow chart.

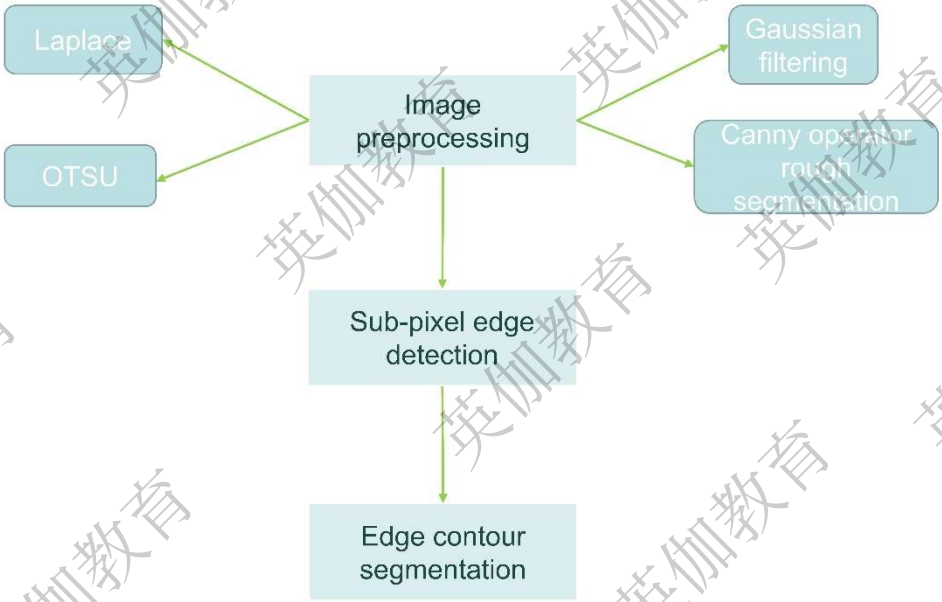

Figure 1 Question 1 flowchart

4.2 For Question 2

When measuring the true length of the given component picture, measurements need to be made according to the calibration version of the given level. The true length

of the provided product image is measured according to the calibration board images of three different angles provided. Image processing requires image preprocessing with OTSU binarization segmentation, Gaussian filtering denoising, image correction, and Canny algorithm segmentation. The image sharpening of the Laplace operator of the part gives the final segmented part segmentation image. Later, the subpixel-level image segmentation of the calibration board and the parts needs to extract the contour edge of the mark point, improve the precision of the center distance measurement, and the parts need to measure the precision to obtain the pixel circumference of each area of the part. Finally, the true length of each part is measured. Observe Figure 2 for the modeling flow chart.

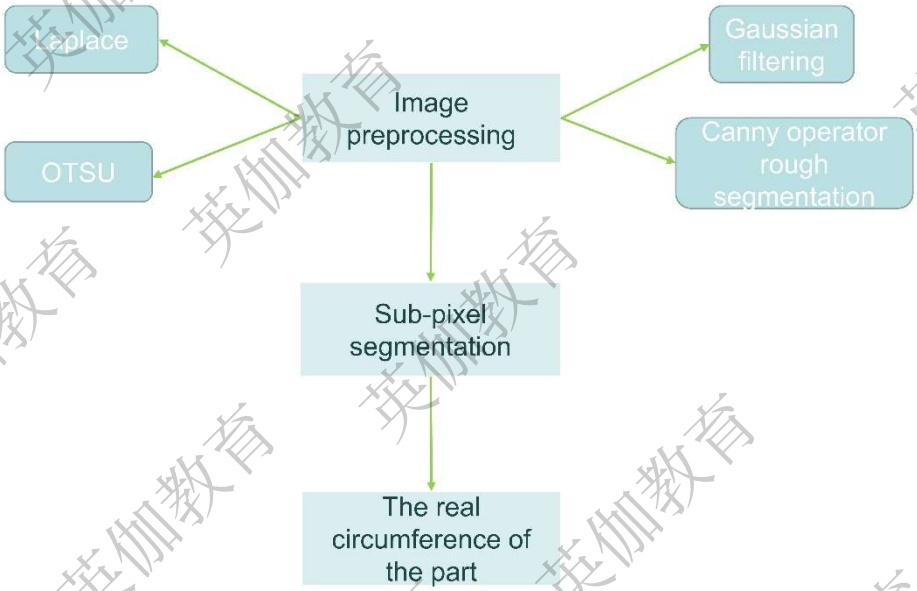

Figure 2 Question 2 flowchart

4.3 For Question 3

Through the two subpixel contour edge data provided in the attachment, model the edge profile segmentation, analyze the edge profile curve data to fit the straight segment, arc segment or ellipse arc segment, find the Edges through Halcon, get the line, circle and ellipse contour according to the read subpixel coordinate data, and finally the center, start position and termination position of the contour everywhere. First, the Ramer algorithm used for contour fitting and data extraction of edge profile. Observe Figure 3 for the flow chart.

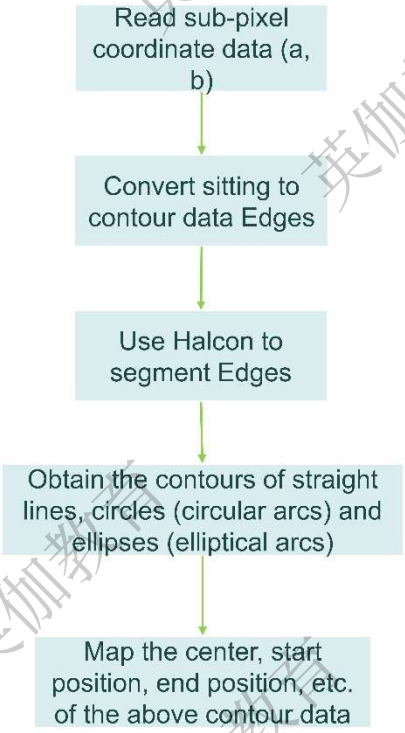

Figure 3 Question 3 flowchart

5. Model Establishment

5.1 Pic1_1 And Pic1_2 Pre-processing

During extracting three image edge profiles, images have noisy image edge profiles, which usually requires edge sharpening and shadow filtering denoising of the image. In this paper, the second derivative of the Laplace operator is used for image sharpening and curvature Gaussian filter denoising. Observe Figure 4 and 5 for the comparison and original images.

Figure 4 Original picture

Figure 5 The Laplace sharpening image

The Laplacian operator is able to enhance the edges and details of the image and improve the contrast. According to the degree of change of the image pixels, when the gray degree of the center pixel in the center pixel of the center pixel, the gray degree of

the center pixel shall be further improved to realize the image sharpening process. When sharpening, it is necessary to derive the relationship between second order differential and pixel, first to measure the first order partial differential method, first order partial differential observe equation (1).

$$\nabla f = \frac{\partial f}{\partial x} + \frac{\partial f}{\partial y} = 2f(x,y) - f(x-1,y) - f(x,y-1) \quad (1)$$

Second-order differential methods can determine the position of the edges, with expressions shown in (2).

$$\nabla^2 f = 4f(x,y) - f(x-1,y) - f(x,y+1) - f\ （x+1,y）- f(x,y-1) \quad (2)$$

This makes the white dots brighter based on the template matrix. Areas where the grayscale jump can be solved, thus making the image clearer.[1]

The contour smoothing operator is the smooth_contours_xld() of the machine vision library. It is often used to calculate distances between profiles. Observe Figure 6 and 7 for contour smoothing operator and contour extraction effects.

Figure 6 Profile smoothing operator processing

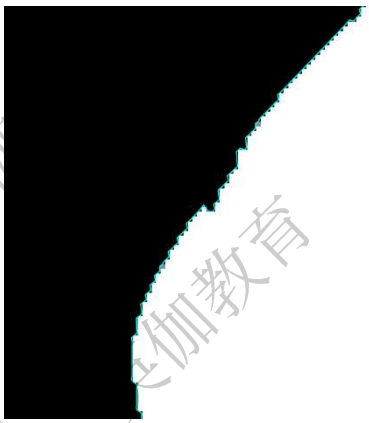

Figure 7 Profile extraction rendering diagram

In image processing, the OTSU method is commonly used for image segmentation-based clustering. The theoretical basis of the algorithm is that the image contains two classes of pixels (foreground and background pixels), the histogram is a bimodal histogram, and then calculates the optimal threshold (intra-class variance) that the two classes can be separated, or the equivalent inter-class variance.

For each coordinate point of the image, the segmentation threshold of the foreground and background is T recorded, the proportion of pixels to the whole image is ω_0, the average gray degree is μ_0; the proportion of background pixels to the whole image is ω_1, the average gray degree is μ_1; the average gray scale of the whole image isμ, and the variance is$g$. Assuming that the image size is $M*N$, the number of pixels in the pixels of the image and the number of pixels less than the threshold is T, the histogram is N_0 obtained from a low valuation between the two peaks. OTSU results for image comparison are shown in Figure 8.

Figure 8 OTSU binarization thresholding segmentation

Denoising was performed using Gaussian filtering. Gaussian filtering is a linear smoothing filter with a good inhibition of noise obeying a normal distribution. Assuming that the noise for this figure is Gaussian white noise, in the pre-processing part of practical application, Gaussian filtering is usually used.

The image was denoised with Gaussian filtering only after the sharpened image and profile were smoothed with the OTSU binarized segmentation process. Gaussian filtering is convolutional using a mask and image, and the template coefficient of the Gaussian filter decreases with the increasing distance from the center of the template. A Gaussian filter maintains the overall details of the image, with the distribution expression shown in (3).

$$f\left(x,y\right)=\frac{1}{\left(\sqrt{2\pi}\sigma\right)^2}e^{-\left((x-ux)^2+(y-uy)^2\right)/2\sigma^2} \tag{3}$$

σCreating a Gaussian filter template where x, y is the coordinate of the image, is the standard deviation of the Gaussian distribution. Its size represents the central coefficient of the generated template. Sampling was performed at the center of the template as the coordinate origin. The coordinates of each position are also brought into the Gaussian function to obtain the coefficient of the filter. Assuming that the size of the resulting window template is (2k + 1) (2k-1), then obtain the calculation formula for each element of the template, observe formula (4).

$$H_{i,j}=\frac{1}{2\pi\sigma^2}e^{-\frac{(i-k-1)^2+(j-k-1)^2}{2\sigma^2}} \tag{4}$$

The calculated results will be in two forms: decimal and integer. Where the form of the decimal number does not need to be processed, the integer form needs to be normalized. After Gaussian filtering processing, the two plots are compared.[2]

Figure 9 Gaussian filter effect map comparison

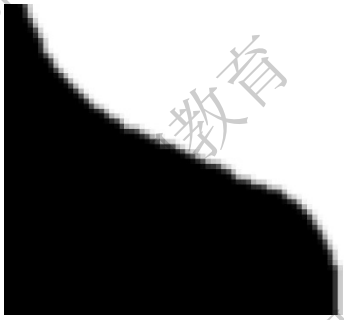

Figure 10 Gaussian filter renderings

Comparing Figure 9 and 10, the profile of the image is clearer after Gaussian filtering processing.

Later, the pixel-level profile of the image is extracted by the Canny operator coarse segmentation for subsequent subpixel edge detection. Effective suppression noise is required to satisfying the coarse segmentation of the Canny operator, smoothing the image using a Gaussian operator and with precise determination of the edge position. After image smoothing and precise edge position respectively using Gaussian filter and OTSU, the time of image edge detection conditions are met, after a three-step processing, first use Gaussian smoothing function to eliminate noise, then use first-order differential convolution template for edge enhancement, and finally use non-maximum inhibition to retain the maximum in the gradient direction. The coarse segmented images are shown in Figure 11.

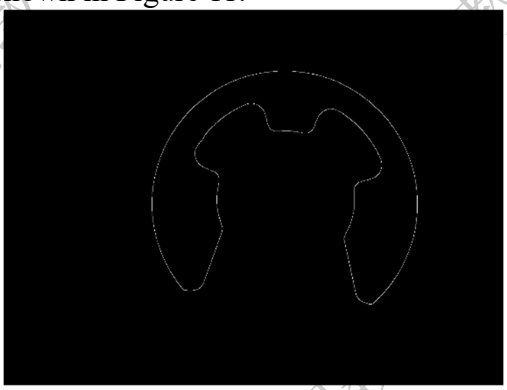

Figure 11 The Canny algorithm for coarse segmentation

Edge enhancement simultaneously obtains both the magnitude of the gradient amplitude and the direction angle, showing differences in the X and Y direction, performing first-order differential convolution operations to obtain the image where the features are enhanced at the edge position. When making a global gradient, it is not enough to determine the edge, to determine the point with the largest local gradient.

5.2 Pic1_3 Image Pre-processing

- Highlight processing of metal artifacts based on the PSO-OTSU algorithm

The area of high reflectivity metal working surface due to the uneven light

distribution, which then affects the visual measurement accuracy. Therefore, we choose the PSO-OTSU algorithm to treat metal artifacts with highlights. First, the highlight regions were extracted using the PSO-OTSU algorithm, secondly using the histogram specification method, and finally fused the processed highlight regions with the original or non-highlight regions to form the de-highlight image.

• The highlight regions were extracted by the PSO-OTSU algorithm

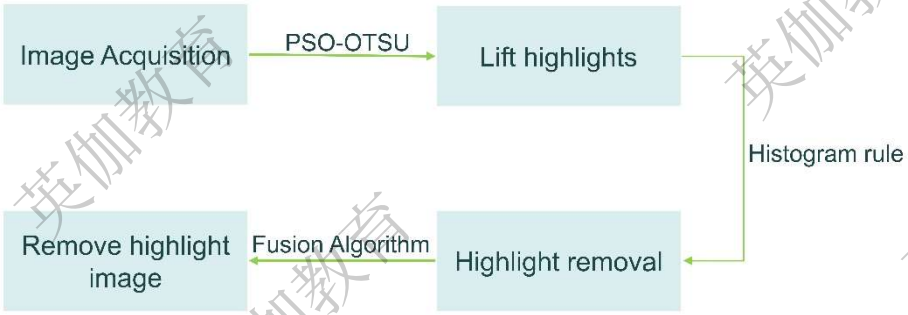

Figure 12 High photosensitive processing process

The PSO-OTSU algorithm is calculated by selecting the fitness function in the P SO algorithm as the maximum inter-class variance criterion. In the process of finding the optimal solution, the particles change the current speed and threshold are based on their own inter-class variance maximum and the global inter-class variance maximum. Until the particles reach the optimal threshold. Observe the iterative algorithm in formula (5).

$$\begin{aligned} V_i^{k+1} &= wV_i^k + c_1 r_1 (pbest_i^k - x_i^k) + c_2 r_2 (gbest_i^k - x_i^k) \\ X_i^{k+1} &= X_i^k + V_i^{k+1} \end{aligned} \tag{5}$$

Where, w for the inertial weight, c_1, c_2 for the acceleration constant, r_1 and r_2 is the random number.

In order to be able to balance the local c_1、c_2 and w global search capabilities, we need to be linearly dynamically adjusted, observe formula for (6), formula for (7).

$$c_1 = 1 + \frac{iter_{now} + 1}{iter_{\max}} \tag{6}$$

$$\begin{aligned} c_2 &= 2 - \frac{iter_{now} + 1}{iter_{\max}(w_{\max} - w_{\min})} \\ w(t) &= w_{\max} - \frac{iter_{now}}{iter_{\max}}(w_{\max} - w_{\min}) \end{aligned} \tag{7}$$

Among them, $iter_{now}$ for the current number of iterations and the maximum number of iterations, the initial value of our parameter is $iter_{\max}$ set according to the standard particle group algorithm, respectively: $w_{\min} = 0.4, w_{\max} = 0.9$, $c_1 = c_2 = 2, iter_{\max} = 20$ learning factor. The resulting de-highlighted images are shown

in Figure 13.

Figure 13 Original picture

Figure 14 After removing the highlights

Figure 15 after binarization using OTSU Oxford method.

Figure 15 Binarization of the OTSU method

• High of area areas based on histogram specification

The implementation of the histogram specification method requires the balanced processing of the original and desired images, and the formula (8),(9),(10).

$$s = \int_0^r P_r(r)\,dr \tag{8}$$

$$v = \int_0^z P_z(z)\,dz \tag{9}$$

$$z = G^{-1}(v) \tag{10}$$

Among them, $P_r(r)$ is the gray degree probability density function of the original image, $P_z(z)$ the gray degree probability density function of the desired image, s the gray level of the original image, v the gray level of the fixed image, and z the gray level of the desired image.

With the above processing, the transformed original image gray scale level can be used to replace the gray scale level of s a given image v .The above inverse transformation analytics is suitable for continuous images. For the discrete images, the prescribed expression is type (11),(12),(13).

$$P_Z(z_k) = \frac{n_k}{n}, 0 \leqslant z_k \leqslant 1 \tag{11}$$

$$v_k = G(z_k) = \sum_{k=0}^{m-1} P_z(z_k) \tag{12}$$

$$z_k = G^{-1}(s_k) \tag{13}$$

Among them, n is the total number of pixels in the image, n_k is the number of k gray scale appearance, m is the number of gray scale level, $P_z(z_k)$ is the probability of k gray scale level.

In conclusion, the histogram regulation method is to reduce the gray degree value of the highlight area by adjusting the gray degree histogram of the highlight area to a predetermined shape.

- Fusion algorithm

A fusion algorithm based on non-highlight region images, which is used as follows:

(1) Find the pixel points of the non-highlight area image is all 0 from the predetermined images and the histograms, and obtain the coordinates of the pixel points; (x_i, y_j)

(2) Find the corresponding pixel point according to the coordinate value, and replace it with the pixel point in the non-highlight area;

(3) The completed replacement image is the final highlight-removed image.

There are multiple scratch noises in the Pic1_3 picture, and the color is similar to the background color, thus leaving blank areas in the components after the binary operation, causing interference with the profile detection. After defect detection and repair processing, an ideal binary image can be obtained for subsequent contour detection. The image were detected by machine vision. The detection of surface defects using deep learning is an end-to-end scheme featuring the convolutional neural network. Its feature extraction ability allows the network to automatically learn the image features of the defect, to understand the defect target from local to global, distributed in different layers of the network, eventually forming the overall perception of the defect target. The advantage is that it more accurately expresses and understands various types of defects than artificial feature extraction, and detects higher precision reading. Its main key lies in the detection algorithm. The temporal image segmentation is used to determine the object type to which each pixel position of the image belongs. Observe Figure 16 for the effect and original drawings.

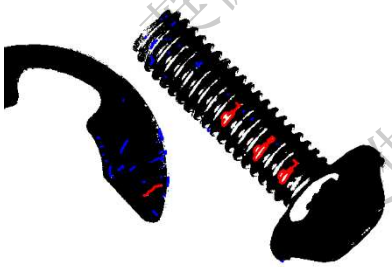

Figure 16 A metal scratch detection image

Blue is short scratch, red is long scratch. After the scratch position of the image is detected, the marked blue-red mark is replaced with black for convenient subsequent step processing to facilitate the extraction of the subsequent profile. The repaired images are shown in Figure 17.

Figure 17 Metal scratch repair image

5.2.1 Product Measurement And Preprocessing

Length measurement of the product requires an image segmentation, separating the part area from the background area. Image segmentation is performed by the threshold segmentation method, and the pixel gray scale amplitude of the product image is divided to divide different grades, and parts regions are extracted by setting the gray scale threshold. Observe (14).

$$g\ （i,j）\ = \begin{cases} 1 & f(i,j) \geq T \\ 0 & f(i,j) < T \end{cases} \tag{14}$$

$g\ （x）\ T$Set as the binary image after the threshold operation; the threshold determined by the gray scale histogram of the image; 1 is the value of the target image; 0 is the value of the background image.

Appropriate thresholds were determined using gray-scale histogram tools in H ALCON. The post-filtered binarized image parts were segmented by the threshold algorithm. According to HALCON, the gray value of the part image is between 0 and 114, and the background image is greater than 114.The operator connection is then divided into different connected domains, and part regions are extracted using area features.[3]

After part binarization processing, the image is denoised. Call open_framegrabber

() with the grab_image_start () operator in the HALCON software. The rgb_to_gray () operator was called to grayscale the image. During image acquisition and transmission, it is not conducive to image processing and analysis, using the median filter operator median_image () and Gaussian filter operators to eliminate pretzel and Gaussian noise by gauss_ image ().

5.2.2 Preprocessing Of The Image Determination

The image determination first requires the calibration board, whose main process is shown in Figure 18.

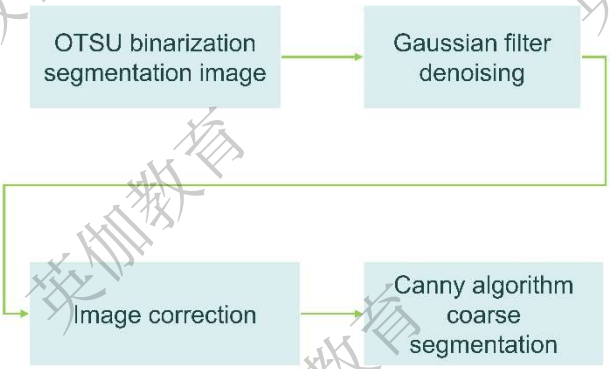

Figure 18 Main process for the calibration board

First considering the OTSU binarization treatment, the basic principle is the same as the first question, except here is to split the circular marker point and the background, used to calculate the pixel length of the center distance of the extracted dot. Comparison of the resulting OTSU binarized images with the original image is shown in Pic2_1 Figure 19 and Figure 20.[4]

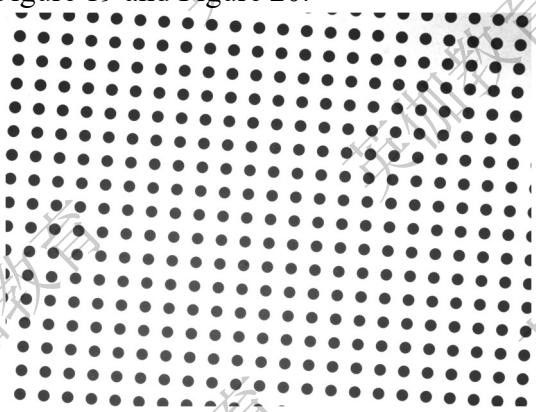

Figure 19 Original picture

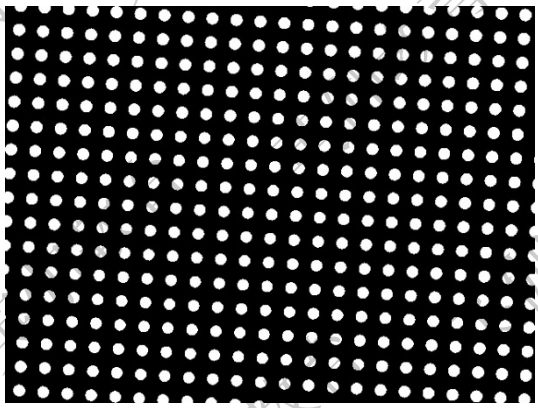

Figure 20 The OTSU binarization processing

The remaining two plots were also treated in the same form.

Afterwards, Gaussian filtering was used to denoise it. Denoising works the same as above, using a Gaussian filter template that then removes the noise on the image. Figure 19 , taken at a non-horizontal angle. Before the image segmentation, the image correction is needed to ensure the precision of the measurement and the collected three scalar images to the horizontal position.

The method of image correction employed is the image area correction. In order to perform the parts work quickly and efficiently and ensure the measurement accuracy, the collected part image needs to be affine and transformed to the horizontal position. The expression for the affine changes is (15).

$$\begin{bmatrix} u \\ v \end{bmatrix} = A \begin{bmatrix} x \\ y \\ 1 \end{bmatrix} = \begin{bmatrix} a_2 & a_1 & a_0 \\ b_2 & b_1 & b_0 \end{bmatrix} \begin{bmatrix} x \\ y \\ 1 \end{bmatrix} \tag{15}$$

Among them, A for the affine transformation matrix, the linear parts and the translation parts composition.

Affine changes mainly include translation transformation and rotation transformation. The translation transformation is to move all the pixels of an image horizontally and vertically at the required offset; while the rotation transformation rotates an image at an angle around a certain point. The expressions for the two are, respectively.

$$\begin{bmatrix} u \\ v \end{bmatrix} = \begin{bmatrix} x \\ y \end{bmatrix} + \begin{bmatrix} x_0 \\ y_0 \end{bmatrix} \tag{16}$$

$$\begin{bmatrix} u \\ y \end{bmatrix} = \begin{bmatrix} \cos\theta & -\sin\theta \\ \sin\theta & \cos\theta \end{bmatrix} \begin{bmatrix} x \\ y \end{bmatrix} \tag{17}$$

Where, respectively, x_0, y_0 is the coordinate translation quantity; θ is the rotation angle.

In HALCON, affine transformation: orientation_region, vector_angle_to_rigid, affine_trans_image. The orientation_region operator is first called to calculate the image deflection angle; then use the vector_angle_to_rigid operator; finally, convert the part image to a horizontal position using the affine_trans_image operator, and the positive Pic2_1 image is shown in Figure 21.

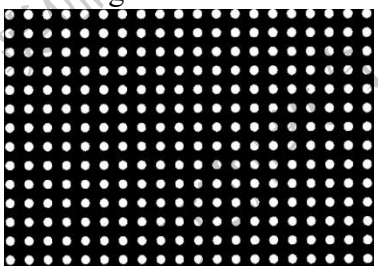

Figure 21 Post-corrected renderings

The corrected image is the same as that taken at a horizontal angle, which can be used as a basis for measuring the part pixels. Finally, the Canny algorithm is coarse divided with the same principle as in the first question. The resulting Pic2_1 images of the Canny algorithm are coarse-segmented in Figure22.

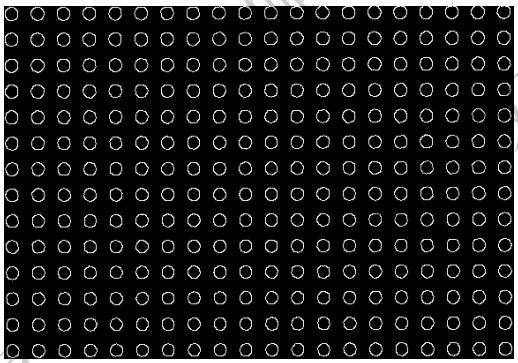

Figure 22 Canny algorithm

6 Problem Solving

6.1 For Question 1

For Pic1_1 and Pic1_2 processing, unlike Pic1_3, Pic1_3 had more noise causing image profile extraction, so the first two plots were processed together. The outline of the first two plots can detect the edge well after preprocessing, and Pic1 _1 and Pic1_2 detect the edge through the Canny subpixels in only four steps:

(1) Smooth the input image with a Gaussian filter;

(2) Calculate the gradient amplitude image and the direction angle image;

(3) Apply non-maximum suppression to the gradient amplitude images;

(4) Detection and connect edges with double threshold processing and connection analysis.

First, to effectively smooth the image and reduce the identification of pseudo-edges, use Gaussian filtering to suppress noise, in the pre-processing has been conducted, a suitable Gaussian filtering standard deviation is important for the effect of edge detection. The parameters of Canny edge detection can be calculated at only the width and height of the edge to the bottom. The Sobel algorithm was selected as the gradient algorithm for the edge detection and extraction process. The finite difference of the first-order bias guide is used to calculate the value of the amplitude of the gradient.

The gradient amplitude is (18).

$$|gradg\ （x,y）|=\sqrt{\left(\frac{\partial g}{\partial x}\right)^2+\left(\frac{\partial g}{\partial y}\right)^2} \tag{18}$$

Do the Sobel algorithm on the image, and each pixel in the image represents the gradient of this point. With the help of Sobel, image preprocessing and segmentation by Canny, and the image are shown in Figure 23 and Figure 24.

Figure 23 Pic1_1 Contour

Figure 24 Pic1_2 Countour

Figure 23 and 24 can clearly observe the contour shape of the two images, after which the edge profile is cut.

Edge profile cutting requires the Ramer algorithm. In fact, recursive segmentation is analyzed in Table 2.

Table 2 for a recursive subdivision

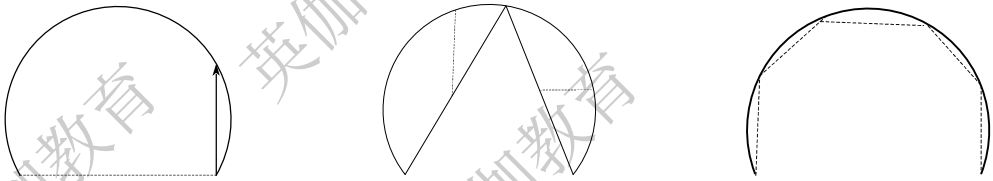

Near polygons are represented by thick lines and then the edges are correctly split apart with the Ramer algorithm for Ramer: the algorithm sometimes places the polygon control point to deviate slightly from the true corner. For this question, these deviations do not pose a problem, due to the maximum accuracy that requires fitting the lines to these contour segments with robust algorithms. Observe Figure 25, Figure 26.

Figure 25 Profile edge segmentation renderings

Figure 26 Profile edge segmentation renderings

For Pic1_3, Pic1_3 image were taken under relatively complex light conditions and with more interference information. Therefore, in the first step, we need to preprocess it, use the Laplace operators and contour smooth operators to complete the image sharpening, remove the edge burr and smooth the contour, to avoid the interference effects caused by the edge hairy edges and shaded parts. Then the PSO-OTSU algorithm was used to remove highlight. Since the three pictures were taken under relatively complex light conditions on the parts, the color of the reflective area is similar to the background color, which will affect the subsequent OTSU binary image

segmentation, so the PSO-OTSU algorithm was used to remove highlight and reduce the effect. Then the OTSU binarization threshold segmentation is used to separate the image foreground from the background, filtering out the background image to easily extract the outline. Gaussian filter is used to remove the noise. For the scratches on the parts, the surface defect detection algorithm and marker feature contour repair are used to obtain the ideal binary image for subsequent contour detection. Observe the resulting contour edge distribution images in Figure 27 and 28.[5]

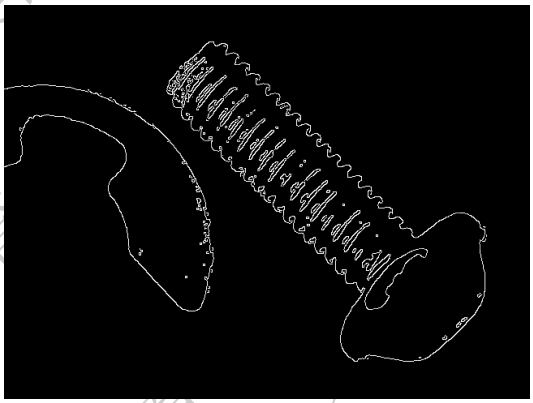

Figure 27 The Canny rough segmentation effect

Figure 28 Edge detection effect

The pixel-level profile of the image was extracted by the Canny operator edge detection algorithm for subsequent subpixel edge detection. The second step regarding subpixel edge detection, we detect edge information using a Gaussian fitting-based subpixel edge detection algorithm. Finally, we use the variable weight least squares based image edge feature extraction algorithm for profile segmentation, observe Figure 29.

Figure 29 Profile cut effect

Finally, the total number of contour curves for Pic1_1 and the number of points and length data on each curve are shown in Table 3.

Table 3 Total number of contour curves for Pic1_2 and the number of points and length on each curve

Total Edge Contours Count:		3610
Total Edge Contours Length:		3183.21
Edge Contour 1	Length	PointCount
	1617.99	1854
Edge Contour 2	Length	PointCount
	55.86	64
Edge Contour 3	Length	PointCount
	154.47	148
Edge Contour 4	Length	PointCount
	136.56	135
Edge Contour 5	Length	PointCount
	60.16	77
Edge Contour 6	Length	PointCount
	268.77	338
Edge Contour 7	Length	PointCount
	61.83	71
Edge Contour 8	Length	PointCount
	109.34	115
Edge Contour 9	Length	PointCount
	51.56	61
Edge Contour 10	Length	PointCount
	259.7	328
Edge Contour 11	Length	PointCount
	69.5	81
Edge Contour 12	Length	PointCount
	138.31	146
Edge Contour 13	Length	PointCount
	151.36	149
Edge Contour 14	Length	PointCount
	47.79	56

The number of edge total contour curves for Pic1_2 and the number of points and length data on each curve are shown in Table 4.

Table4 Total number of contour curves for Pic1_2 and the number of points and length on each curve

Total edge profile count	7970	
Total edge contour length	6763.46	
Edge Contour 1	Length 346.82	PointCount 403
Edge Contour 2	Length 955.34	PointCount 1099
Edge Contour 3	Length 205.74	PointCount 266
Edge Contour 4	Length 163.64	PointCount 200
Edge Contour 5	Length 173.07	PointCount 205
Edge Contour 6	Length 79.56	PointCount 100
Edge Contour 7	Length 188.74	PointCount 247
Edge Contour 8	Length 81.59	PointCount 114
Edge Contour 9	Length 69.64	PointCount 82
Edge Contour 10	Length 76.38	PointCount 78
Edge Contour 11	Length 249.16	PointCount 317
Edge Contour 12	Length 251.56	PointCount 280
Edge Contour 13	Length 497.51	PointCount 530
Edge Contour 14	Length 62.3	PointCount 72
Edge Contour 15	Length 170.78	PointCount 226
Edge Contour 16	Length 67.97	PointCount 83
Edge Contour 17	Length 385.82	PointCount 441
Edge Contour 18	Length 142.11	PointCount 177

Edge Contour 19	Length 422.99	PointCount 534
Edge Contour 20	Length 273.61	PointCount 333
Edge Contour 21	Length 64.29	PointCount 88
Edge Contour 22	Length 139.93	PointCount 144
Edge Contour 23	Length 77.39	PointCount 83
Edge Contour 24	Length 208.56	PointCount 252
Edge Contour 25	Length 169.82	PointCount 200
Edge Contour 26	Length 78.7	PointCount 77
Edge Contour 27	Length 137.29	PointCount 136
Edge Contour 28	Length 73.74	PointCount 85
Edge Contour 29	Length 349.37	PointCount 399
Edge Contour 30	Length 107.77	PointCount 132
Edge Contour 31	Length 172.65	PointCount 215
Edge Contour 32	Length 136.63	PointCount 159
Edge Contour 33	Length 182.99	PointCount 238

The representations of the total outline technique and length are shown in Table 5.

Table5 Total edge profile counts and length of Pic1_3

Total edge profile count	194
Total edge contour length	6870.37

6.2 For Problem 2

Subpixel segmentation of the image is required before making the image measurements. Subpixel segmentation is mainly to extract contour edges of marker points and improve the precision of center distance measurements. The algorithm used is for the calibration board to improve the measurement accuracy of the image of each area of each part. The process of extracting the edge and line characteristics of the large spatial direction of the gray value is edge detection. In this paper, a gradient is used to

reflect the edge position of the image, and the gradient of $f(x,y)$ a continuous image function is expressed as (19).[6]

$$\nabla f(x,y) = [G_x \quad G_y]^T = \left[\frac{\partial f}{\partial x} \quad \frac{\partial f}{\partial y}\right]^T \tag{19}$$

Part image edges were extracted by using the edge detection of the Canny operator. The basic principle is to first select a Gaussian filter to smoothly filter the image, and then use the non-extreme suppression technology to obtain the image edge. The steps are as follows.

First: smooth the image by using $f_s(x,y)$ a circular 2D Gaussian filter to smooth $G(x,y)\, f(x,y)$.

$$G(x,y) = e^{\frac{x^2+y^2}{2\sigma^2}} \tag{20}$$

$$f_s(x,y) = G(x,y) \cdot f(x,y) \tag{21}$$

Second: calculate the gradient amplitude $M(x,y)$ and direction of $\alpha(x,y)$ each pixel of the smooth image, and the edge emphasis and direction of each point are calculated using the gradient amplitude and direction.

$$M(x,y) = \sqrt{(g_x)^2 + (g_y)^2} \tag{22}$$

$$\alpha(x,y) = \arctan\left(\frac{g_x}{g_y}\right) \tag{23}$$

Third: perform the non-maximum suppression of the gradient amplitude to determine the point with the largest local gradient and the inhibition non-maximum, the non-local maximum point is set to 0 to refine the edge.

Fourth: set the low and high threshold to detect the edges T_1 and T_2 the connected edges by comparing the edge pixels of the image with the set high and low threshold. The images obtained from segmentation according to the Canny algorithm are shown in Figure 30.

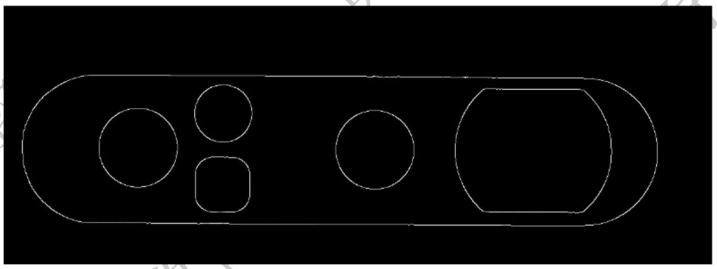

Figure 30 The Canny algorithm for coarse segmentation

Following the above principles, we extracted the subpixel edges of the part images.

The resulting image edges are shown in Figure 31.

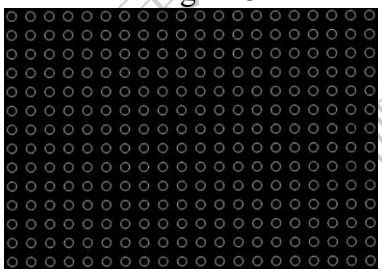

Figure 31 Subpixel edge detection rendering

After subpixel edge detection, image edges were performed. Image edge extraction included linear fitting and circle fitting. Where the line fitting is performed by calling the select_shape_xld()operator in HALCON, using the characteristic histogram of XLD to remove the aperture edge using the width, retaining only the outer outline of the part. The segment_contours_xld() operator is then called for segmentation, and the segmented profile is determined by the global profile attribute cont_approx.

After the part profile segmentation is completed, calling the get_contour_global_attrib_xld() operator obtains the properties of each profile. When Attrib = -1 belongs to the line segment, the fit_line_contour_xld () can fit the boundary value of the image to obtain the actual size of the part according to the conversion relationship.

Sometimes the aperture of the shot part can not obtain the complete circular outline during the edge extraction, which may be due to shooting instability or field environment, so the arc, which is not conducive to the fitting of the circle, so we combined the arc and call the union_cocircular_contours_xld() operator to combine the arc.

In this paper, the circle parameter is fitted by least squares, so fitting the circle does not affect even the edge localization and detection. The expressions of the circle equation is (24).

$$(x-x_0)^2+(y-y_0)^2=r^2 \tag{24}$$

The minimum sum of square of error of the objective function is (25).

$$S=\sum_{i=1}^{n}\left[\sqrt{(x_i-x_0)^2+(y_i-y_0)^2}-r\right]^2 \tag{25}$$

These are the coordinates of $(x_i,y_i),i=1,2,3$ the feature points on the arc n in the image coordinate system and the number of feature points involved in the fitting.

To obtain a direct solution to a minimization problem, while avoiding the square root, the objective function can be overwritten as (26).

$$E=\sum_{i=1}^{n}\left[(x_i-x_0)^2+(y_i-y_0)^2\right]^2 \tag{26}$$

To sort out the top formula (27).

$$E=\sum_{i=1}^{n}\left(x_i^2-2x_0x_i+x_0^2+y_i-2y_0y_i+y_0^2-r^2\right)^2 \tag{27}$$

a surname $B=-2y_0,\ A=-2x_0,\ C=x_0^2+y_0^2-r^2$

The upper formula can be expressed as (28).

$$E=\sum_{i=0}^{n}\left(x_i^2+y_i^2+Ax_i+By_i+C\right)^2 \tag{28}$$

According to the principle of E least squares, the conditions to be met to A,B,C solve the minimum are (29),(30),(31).

$$\frac{\partial E}{\partial A}=2\sum_{i=0}^{n}\left(x_i^2+y_i^2+Ax_i+By_i+C\right)x_i=0 \tag{29}$$

$$\frac{\partial E}{\partial B}=2\sum_{i=0}^{n}\left(x_i^2+y_i^2+Ax_i+By_i+C\right)y_i=0 \tag{30}$$

$$\frac{\partial E}{\partial C}=2\sum_{i=0}^{n}\left(x_i^2+y_i^2+Ax_i+By_i+C\right)=0 \tag{31}$$

Solving the above three formulas, the fitting value of the center coordinate (x_0,y_0) and r radius is (32).

$$x_0=-\frac{A}{2},y_0=-\frac{B}{2},r=\frac{1}{2}\sqrt{A^2+B^2-4C} \tag{32}$$

For curve fitting and circle fitting processing, the components can be detected by subpixel edges. The resulting component effect 31 is compared with the original Figure 32.

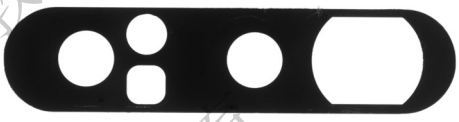

Figure 32 Original picture

Figure 33 Subpixel edge detection effect diagram of the components

This is then the need to measure the length of the part. First, we can find the pixel distance. Then according to the (33).[9]

$$\frac{I_i}{I_k}=\frac{Z_i}{Z_k} \tag{33}$$

The (33) I_i represents the pixel value corresponding to the two centers of Z_i the calibration plate, I_k the real distance of the calibration plate, $Z_k$and the real distance of the calibration plate.

The real length represented is Z_i known to be 2mm, given the pixel values and the mean values of the three images.

Table 6 Calibration plot center distance

order number	Pic2_1	Pic2_2	Pic2_3	average
The center distance	58.8742	58.2367	59.3419	58.8176

The same algorithm is adopted to measure the contour pixels of parts and the data are shown in Table 7.

Table 7 Contour pixel length

order number	1	2	3	4	5	6
length	4532	436.349	321.472	329.124	437.874	834.231

Enter Type (33) for the true length value of the outline, observe Table 8.

Table 8 Edge contour length output format (mm)

Contour ID	Length(mm)
Total Edge Contours	234.3193
Edge Contour 1	154.1035
Edge Contour 2	14.8374
Edge Contour 3	10.9311
Edge Contour 4	11.1913
Edge Contour 5	14.8892
Edge Contour 6	28.3667

The desired length is the true length of the required profile.

6.3 For Question 3

6.3.1 Allocation Method Of Power At The Inflection Point

Using the general weight assignment method, some non-near points will have a large weight at the inflection point. Considering the geometric characteristics of the closed discrete point, this paper uses the curve fitting method to calculate the weights at the inflection point.

x_{i+1} and x $x_1=x$ definition between two adjacent x_i discrete points (x_1,y_1), $w(s(x_i))$ takes a point on two lines, so that the weights of each point in the support domain are determined by the distance between the point to the point, and type(34).

$$s(x_i)=\frac{\sqrt{(x_1-x_i)^2+(y_1-y_i)^2}}{k\max\left(\sqrt{(x_1-x_j)^2+(y_1-y_j)^2}\right)} \tag{34}$$

Among $i,j=1,2,\cdots,N,k>1$.

The distance from discrete to point (x_1,y_1) within the support domain determines the radius of the support domain, and reasonable selection values can determine that the weights of $w(s(x_i))$ each point in the support domain are in the decay region of the weight function, and control the degree of local approximation of the curve. The assignment of such weights is x related to the geometric characteristics of the discrete point at the corner, supporting the gradual decay along the two directions of the domain, and ensuring the approximation nature of the fitting curve at the corner.

In these two cases, the calculation formulas are (35),(36).

$$y_1=\frac{x_1-x_i}{x_{i+1}-x_i}(y_{i+1}-y_i)+y_i \tag{35}$$

$$y_1=\frac{x_1-x_{i+1}}{x_i-x_{i+1}}(y_i-y_{i+1})+y_{i+1} \tag{36}$$

7 Test Of The Model

7.1 Model Checking Of The First Question

This article compares the five sub-pixel edge detection algorithms of Gaussian fitting, spatial matrix, Zernike moment method, OFMM method, and PZM method to detect the positioning accuracy and the running time of the detection, observe the Table 9.

Table 9 The detection results of several sub-pixel edge detection algorithms for step-shaped edges

	Gaussian fitting	Space matrix method	Zernike matrix	OFMM	PZM method
Positioning accuracy/pixel	0.084	0.141	0.115	0.102	0.187
Detection time/ms	103	142	1.5	130	109

It can be seen from the table that the positioning accuracy of the sub-pixel edge detection algorithm based on Gaussian fitting is higher than that of the sub-pixel edge detection algorithm based on spatial matrix, Zernike moment method, OFMM method, and PZM method. And the detection based on the sub-pixel edge detection algorithm takes the shortest running time, so its efficiency is the highest.[10]

7.2 Model Checking Of The Second Question

The starting and ending point coordinates of the part boundary are obtained by straight line fitting, the image_points_to_world_plane() operator is adjusted in HALCON to convert the image coordinates of the starting and ending points of the straight line into world coordinates, and the distance_pp() operator for calculating the distance between two points is called to obtain the actual side length of the part . Let x represent the actual size and p represent the distance of 1 pixel in the image. Through the obtained pixel coordinates and world coordinates of the circular mark of the HALCON calibration board, combined with the result of the camera calibration, the actual size corresponding to each pixel is 0.00011 mm. In order to obtain the actual size of the aperture r. Use high-precision measuring equipment to measure the actual size of the part, compare it with the visual measurement result and calculate the error.

Table 10 Operation time of 3 methods

	L_1	L_2	L_3	L_4	radius
Actual size /mm	30.012	74.987	29.989	75.011	5.000
measure size /mm	30.023	75.004	30.005	74.994	4.991
error /mm	-0.011	-0.017	-0.016	0.017	0.009

It can be seen from the table that the size of the parts measured by vision is very small from the actual size, and the error of each size is within ± 0.02 mm, which satisfies the acceptable error range, and the accuracy and real-time performance meet the inspection needs of industrial production.[11]

8 Extension And Evaluation Of The Model

8.1 Extension Of The Model

For the shortcomings of Sobel algorithm, this algorithm makes two improvements

based on the classical Sobel algorithm to compensate for the shortcomings of Sobel algorithm.

8.1.1 Direction Templates Are Set To 8

The edge of the image has many directions. In addition to the horizontal and vertical directions, there are other edge directions, such as 600, 1200, etc.

8.1.2 Use The Edge Tracking To Discharge The Noise Points

After the calculation of the 8-point orientation template and the determination of the threshold value, we detected the pixels with the new gray-scale values greater than or equal to the threshold value. However, it is not possible to determine that these pixels are the edge points, because the noise also causes a jump in the pixel gray degree, resulting in new gray values greater than or equal to the threshold value. Therefore, the corresponding method must be further taken to determine whether the pixel is an edge point or a noise point, and the edge tracking method is adopted to determine below.

8.1.3 Basic Ideas Of Edge Tracking

The edge has two features of direction and amplitude, perpendicular to the edge direction, and the pixel gray value changes dramatically, while the pixel gray value changes gently along the edge direction[8]. The edges of the object are continuously smooth, and along either edge point, another edge point with a small difference in gray value and direction can always be found. However, the noise is different. Because the noise is random, it is difficult to find another noise point with a small difference in the gray degree value and direction along the edge direction. Using this basic idea, the actual edge point can be distinguished from the noise point. In order to more accurately determine whether a pixel is an edge point, the pixels are generally tracked continuously along the edge direction.[12]

8.2 Evaluation Of The Model

8.2.1 Merit

1.Sobel usually has a larger absolute value for the elements of the output image (array);

2. The detection method has a good effect on the image processing with more gray scale gradient and more noise;

3. Can identify as many actual edges in the image as possible;

4. The identified edges should be as close as possible to the actual edges in the actual image;

5. Provide more accurate edge direction information.

8.2.2 Shortcoming

Disadvantages of Sobel algorithm Because the edge is a sign of position, they are not sensitive to the change of gray scale.

9 Reference

[1] Gu Tianqi, Zhang Lei, Ji Shijun, Tan Xiaodan, Hu Ming.Curve fitting method for closed discrete points [J].Journal of Jilin University (Engineering Edition), 2015,45(02):437-441.DOI:10.13229/j.cnki.jdxbgxb 201502015.

[2] Lin Haibo, Pan Wanui.Research and application of the image edge feature extraction algorithm [J].Combined machine tool and automatic processing technology, 2015(06):118-120.DOI:10.13462/j.cnki.mmtamt.2015.06.032.

[3] Han Dong, Li Yuqi, Wu Yanhui.Sub-pixel edge detection algorithm based on a Gaussian fitting [J].Computer applications and Software, 2018,35 (06): 210-213 + 229.

[4] Gao Maoyuan, Wang Haochen, Cong Zhiwen, Wang Zezheng, Li Jiapeng.Fast and precision measurement of mechanical part dimensions based on HALCON [J].Electromechanical Engineering technology, 2020,49 (03): 71-74 + 127.

[5] Tang Song, Yang Qihua, Liu Gang.Sub-pixel level of core size measurement based on Halcon [J].Computer Engineering and Application, 2017,53 (03): 237-241.

[6] Chen Yifeng. Application of Halcon on artifact 2 D size detection [J].Electromechanical technology, 2011,34 (04): 12-13 + 17.

[7] Cai Yan, Ye Lianxiang, Sun Dawei, Tian Hua, Zhu Junjie, Hu Zhiyun. Based on an improved Zernike moment subpixel edge extraction algorithm for external threaded non-contact measurements [J].Journal of Shanghai Jiao Tong University, 2014,48(10):1468-1472+1478.DOI:10.16183/j.cnki.jsjtu.2014.10.021.

[8] Lu Zhengqi, Han Yongxiang, Liu Yubao. Improving the Ramer scheme for diagnosis of freezing rain in China[J].Atmospheric Research,2021,254:

[9] Elworthy K.D..Infinite-Dimensional Degree Theory and Ramer'S Finite Co-Dimensional Differential Forms[J].The Quarterly Journal of Mathematics,2021,72(1-2):

[10] Chen Fangsheng, He Chunyu, Chen Yafei. Improving application of Canny algorithm in thickness edge detection [J].Steel rolling, 2021,38(05):81-85.DOI:10.13228/j.boyuan.issn 1003-9996.20210514.

[11] Yuan Weiqi, Zhao Peiyao. Adaptive heat exchanger plate edge detection method based on Canny [J].Computer Technology and Development, 2021,31 (11): 81-85 + 94.

[12] Fei Jiyu, Wang Zheng, Li Hua, Liu Zhibo, Jiang Wei, Liu Xiaodong, Zhang Junfei. Metal artifact highlight processing based on the PSO-OTSU algorithm [J].Journal of Dalian Jiaotong University, 2020,41(03):28-33.DOI:10.13291/j.cnki.djdxac.2020.03.006.